Desalination and Water Treatment
www.deswater.com

doi: 10.1080/19443994.2015.1062433

57 (2016) 14178–14187
June

Taylor & Francis
Taylor & Francis Group

TiO_2-nanostructured carbon composite sorbent/photocatalyst for humic acid removal from water

Corina Orha[a], Florica Manea[b,*], Aniela Pop[b], Cornelia Bandas[a], Carmen Lazau[a]

[a]*Condensed Matter Department, National Institute for Research and Development in Electrochemistry and Condensed Matter, Timisoara, P. Andronescu no. 1, 300254 Timisoara, Romania, emails: haiduccorina@yahoo.com (C. Orha), cornelia.bandas@gmail.com (C. Bandas), carmen.lazau@gmail.com (C. Lazau)*

[b]*Department of Applied Chemistry and Engineering of Inorganic Compounds and Environment, Politehnica University of Timisoara, V. Parvan Bd., no. 6, Timisoara 300223, Romania, Tel. +40 256/403071; Fax: +40 256/403069; emails: florica.manea@upt.ro (F. Manea); email: aniela.pop@upt.ro (A. Pop)*

Received 3 March 2015; Accepted 9 June 2015

ABSTRACT

In this study, two types of nanostructured carbon–TiO_2 within epoxy matrix, i.e. carbon nanotubes-TiO_2-Epoxy (CNT-TiO_2-Epoxy) and carbon nanofiber-TiO_2-Epoxy (CNF-TiO_2-Epoxy) have been prepared, characterized and tested as sorbent and photocatalysts for humic acids (HAs) removal from water envisaging advanced drinking water treatment. The HA adsorption capacities of CNT-TiO_2-Epoxy of 8.68 mg g^{-1} and CNF-TiO_2-Epoxy of 7.14 mg g^{-1} were determined using Freundlich isotherm and pseudo-second-order kinetics model. Also, the photocatalytic activities of both composites were assessed in terms of HA degradation efficiency and rate constant and an enhancement effect was found for CNT-TiO_2-Epoxy composite for HA removal. CNF-TiO_2-Epoxy photocatalytic performance was worse vs. simple TiO_2 traditional catalyst in terms of degradation efficiency, but five times faster from the kinetics point of view. The lifetime and the regeneration pathway by the photocatalysis were assessed for CNT-TiO_2-Epoxy composite system in comparison with the sorption applications. A HA removal efficiency of 43.8% was found by photocatalysis vs. 30.2% reached by the sorption after successive five running. A regeneration degree of about 25% was achieved under the similar conditions of photocatalysis without HA presence.

Keywords: Carbon materials; Titanium dioxide; Humic acid; Sorption; Photocatalysis

---

1. Introduction

Natural organic matters (NOM) in the surface water derived from the degradation of plants and micro-organisms. Humic acids (HAs) represent a large portion of NOM present in most surface water used for drinking [1] and also, in sediments and soils [2]. Removal of HAs has long been of concern in water treatment due to their diverse reactivity and abundance in natural waters [3].

Chlorination, the most widely used disinfection technique to destroy pathogens in drinking water could lead to the formation of trihalomethanes and other toxic by-products in the presence of NOM, and this aspect represents one of most important reason

---

*Corresponding author.

for NOM removal from water [4]. Also, presence of NOM in drinking water source is responsible for membrane fouling in ultra- or nano-filtration steps of the drinking water treatment technology. For this reason, numerous approaches have been investigated for the development of cheaper and more effective materials characterized by advanced properties suitable for the adsorption and photocatalysis applications in the water treatment. Various carbonaceous materials, e.g. activated carbon [5], carbon nanotubes (CNTs) [6] and carbon nanofibers (CNFs) [7] have been intensively tested as sorbents, composite filters, antifouling membranes and photocalysis processes [8–10]. Moreover, CNTs have been demonstrated as excellent catalyst support and as building block in hybrid catalyst to improve the photocatalysis performance of the traditional photocatalyst, such as TiO_2 [11].

Carbon nanomaterials have been used as a support for the dispersion of the functional materials in order to give them additional functional properties, such as: structure, surface area, activity and conductivity. Carbon particles have been used for the photocatalytic composite for many purposes, e.g. adsorbent agents, dispersants for avoiding photocatalyst agglomeration and increment of the effective surface area [12,13]. Nanostructured carbon composite materials are used for interesting applications in many fields due to their unique properties compared to bulk material and have been the subjects of numerous studies [14–16].

Composite materials containing carbon and TiO_2 have been tested for many applications, e.g. treatment of contaminated water and air by the heterogeneous photocatalysis, hydrogen evolution, CO_2 photoreduction, dye sensitized solar cells and sensor devices [17], exhibiting cooperative and synergetic effects between the metal oxides and carbon phases. Some recent works have emphasized on the preparation of these new hybrid materials and a few examples are reported [18–21]. These composite materials have been fabricated by a range of different methods, including mechanical mixing of TiO_2 and carbon materials [22], sol–gel synthesis of TiO_2 in the presence of carbon [23], electro-spinning methods [24,25], electrophoretic deposition [26] and chemical vapour deposition [27]. Titanium dioxide is a traditional inexpensive photocatalyst material using UV irradiation to degrade environmental pollutants from industrial wastewater owing to its ability to convert them into innocuous end products such as CO_2 [12,28–30].

The mixture of titanium dioxide and carbon materials provides an effective surface area, where pollutants (organic or inorganic compounds) can be adsorbed and destroyed photocatalytically. Adsorption is a key process in the photocatalytic destruction of the pollutants and TiO_2-carbon particles composites are able to achieve enhanced photocatalytic activities [31].

Even if much progress has been made recently, in adsorption and photocatalysis applications of CNTs and CNT-TiO_2 [11], however, there is still a lot of works to do to enhance its performance in water treatment. Several drawbacks must be taken into considerations: (a) the aggregation of CNTs in aqueous solution limits the available sites for the adsorption of the pollutants; (b) the small size of CNTs makes them to be difficult to separate from aqueous solutions and energy-consuming methods are required, e.g. ultracentrifugation and membrane filtration. In this context, CNFs are considered as alternative for CNTs because they possess similar adsorptive and electron properties and are cheaper and easier to manipulate [32].

The aim of this work is to investigate comparatively the performances of two types of composite materials, e.g. carbon nanofiber-TiO_2-Epoxy (CNF-TiO_2-Epoxy) and carbon nanotubes-TiO_2-Epoxy (CNT-TiO_2-Epoxy) for adsorption and photocatalytic degradation of HAs from water envisaging drinking water treatment improvement. The main idea is to use a simple, cheap and efficient method for the preparation of a composite system that achieves a good dispersion of nanostructured carbon and TiO_2 nanoparticles allowing their easy separation after the practical application in water treatment technology. Two approaches regarding CNT/CNF-TiO_2 composite are considered, the first is linked to the effect of TiO_2 on adsorption process of HA involving the regeneration of fouled adsorbent. The second approach is regarded to the photocatalytic activity of these composites that should be enhanced vs. TiO_2 because of the potential effect of CNT/CNF to retard the electron–hole pair recombination [33]. A potential synergic effect between nanostructured carbon and TiO_2 related to the photocatalytic activity is confirmed in this study.

2. Experimental

2.1. Materials and composite materials preparation

Multiwall CNTs and CNF were purchased from Nanocyl, Belgium (Belgium Nanocyl, Sambreville, Belgium) and respective, from Sigma-Aldrich, St. Louis, USA. CNT are characterized by high specific surface area of $500\ m^2\ g^{-1}$ vs. $65–75\ m^2\ g^{-1}$ for CNF. Titanium dioxide TiO_2 nanocrystals were synthesized by sol–gel method [34].

For the synthesis process of the composite materials consisted of CNTs or CNFs mixed with TiO_2 particles within epoxy matrix, the two-roll mill technique was applied. The composite materials were prepared by dispersion of CNTs and CNFs in tetrahydrofuran 99.9% (THF, Sigma-Aldrich, Germany) and epoxy resin (Araldite®LY5052, Huntsman Advanced Materials, Basel, Switzerland) by ultrasonication for 20 min, followed by the homogenization of the resulting paste with the TiO_2 particles and also, with the hardener using a two-roll mill to obtain a high level of dispersion and homogeneous distribution of the components in the epoxy matrix. The ratios were chosen to reach 20% (wt.) carbon, 20% (wt.) TiO_2 and respective, 60% (wt.) epoxy.

For adsorption and photocatalysis application, the composite material was crushed and sieved and the composite size between 1 and 2 mm was used. The HA was obtained from Sigma Aldrich, Switzerland, and 100-mg L^{-1} stock solution of HA was prepared by dissolving 0.1 g of HA in 1,000 ml of distilled water. All experiments were performed at pH of 6.5.

2.2. Characterization of the composite material

A scanning electron microscopy (SEM) using Inspect S PANalytical model coupled with the energy dispersive X-ray analysis detector was used to characterize the morphology of the composite materials, using catalyst powder supported on carbon tape. The light absorption properties of the composite materials were studied by UV–vis Diffuse Reflectance Spectroscopy (DRUV–vis), performed under ambient conditions using Lambda 950 Perkin–Elmer device in the wavelength range of 200–650 nm.

Zeta potential measurements were carried out by a Zeta Meter 3.0+ for suspensions of 1 g L^{-1} composite material in distilled water at pH of 6.5.

2.3. Adsorption and photocatalysis experiments

Both TiO_2-carbon composite materials, i.e. CNT-TiO_2-Epoxy and CNF-TiO_2-Epoxy were tested as adsorbents and photocatalysts in advanced water treatment processes for the removal of HAs from water.

To study HA sorption and photocatalytic activity, an accurate weight of 0.3 g of composite materials were shaken with 300 mL of 10, 15, 20 and 25 mg L^{-1} HA solutions for 180 min at pH of 6.5. The experimental solution was prepared by diluting the HA stock solution with distilled water.

The photocatalytic experiments were carried out under magnetic stirring at 20˚C into a RS-1 photocatalytic reactor (Heraeus, Germany), which consisted of a submerged UV lamp surrounded by a quartz shield. The adsorption of HA on composite materials was studied using batch method in the same photocatalytic reactor without UV irradiation to achieve the same hydrodynamic conditions. After irradiation time of 3 h, the suspension was sampled and filtered through a 0.2 mm membrane filter. The concentration of HA was measured in terms of absorbance at 254 nm (A_{254}) with a Carry 100 Varian spectrophotometer.

For all studied processes, the HA removal efficiency was calculated using the following equation:

$$\text{Removal efficiency } = \frac{C_0 - C_t}{C_0} \times 100\,(\%) \tag{1}$$

where C_0 and C_t are the concentrations of HA in aqueous solution at initial time and at any time t, respectively, (mg L^{-1}).

Kinetics data were fitting with the pseudo-second-order kinetic model [35] expressed as (Eq. (2)):

$$\frac{t}{q_t} = \frac{1}{k_2 q_e^2} + \frac{t}{q_e} \tag{2}$$

where k_2 is the rate constant of the pseudo-second-order adsorption kinetics (g mg^{-1} min^{-1}); q_e—the equilibrium adsorption capacity (mg g^{-1}).

From the kinetics point of view, for the heterogeneous photocatalytic processes, the dependencies of the HA degradation rate on the irradiation time have been described by the Langmuir–Hinshelwood kinetic model [36] (Eq. (4)), which can be simplified to a pseudo-first-order equation (Eq. (3)):

$$r = \mathrm{d}C/\mathrm{d}t = kKC/(1 + KC) \tag{3}$$

$$\ln(C_0/C_t) = kKt = k_{\mathrm{app}}t \tag{4}$$

where r is the rate of HA degradation and discoloration (mg L^{-1} min^{-1}); C_0 is the the initial HA concentration (mg L^{-1}); C_t is the concentration of the HA at time t (mg L^{-1}); t is the irradiation time (min); k is the reaction rate constant (min^{-1}).

The apparent rate constant, k_{app}, was calculated from the intercept of the plot of $\ln(C_0/C_t)$ vs. time, t.

For equilibrium study regarding HA adsorption on the composite materials, three models presented below were applied to assess the adsorption isotherm:

The linear form of the *Langmuir isotherm* can be represented by the following Eq. (5):

$$\frac{1}{q_e} = \left(\frac{1}{K_{\mathrm{L}} q_m}\right) \frac{1}{C_e} + \frac{1}{q_m} \tag{5}$$

where C_e is the equilibrium HA concentration at 30 min adsorption time (mg L^{-1}); q_m is the maximum adsorption capacity (mg dye/g zeolite); K_L is the Langmuir isotherm constant (L g^{-1}).

The *Freundlich equation* for a linear plot is described by the following Eq. (6):

$$\ln\ q_e = \ln\ K_F + n\ \ln\ C_e \tag{6}$$

where K_F is the Freundlich constant (L g^{-1}); n is the heterogeneity factor.

The *D-R equation* is expressed in a linear form as (Eq. (7)):

$$\ln\ q_e = \ln\ q_m - K_{DR}\varepsilon^2 \tag{7}$$

where q_m is the monolayer capacity (mol kg^{-1}); ε is the Polanyi potential equal to $RT\ln(1 + 1/C_e)$; R is the gas constant (J mol^{-1} K^{-1}); T is the absolute temperature (K); K_{DR} is the constant of the adsorption energy (mol^2 J K^{-1}).

3. Results and discussion

3.1. Scanning electron microscopy (SEM)

Fig. 1(a) and (b) shows the SEM images of CNT-TiO_2-Epoxy and CNF-TiO_2-Epoxy composite material. It can be noticed that part of TiO_2 nanoparticles was attached on CNT/CNF surface and also, a well dispersion of nanostructured carbon and TiO_2 nanoparticles within epoxy matrix is noticed. A more uniform distribution of TiO_2 nanoparticles seems to appear for CNF in comparison with CNT.

3.2. DRUV–vis spectroscopy

The diffuse reflectance UV–vis spectra of CNT-TiO_2-Epoxy and CNF-TiO_2-Epoxy in comparison with of CNT-Epoxy, CNF-Epoxy and TiO_2 are presented in Fig. 2, expressed in terms of Kubelka-Munk equivalent absorption units. It is observed for both CNTs and CNFs an increased absorption in VIS wavelength range in comparison with single TiO_2 that absorb only in UV wavelength range, which informs about the potential of CNTs- and CNFs-based materials to be used in VIS-driven photocatalysis applications. However, the absorption intensity at VIS wavelength is lower towards UV absorption, and

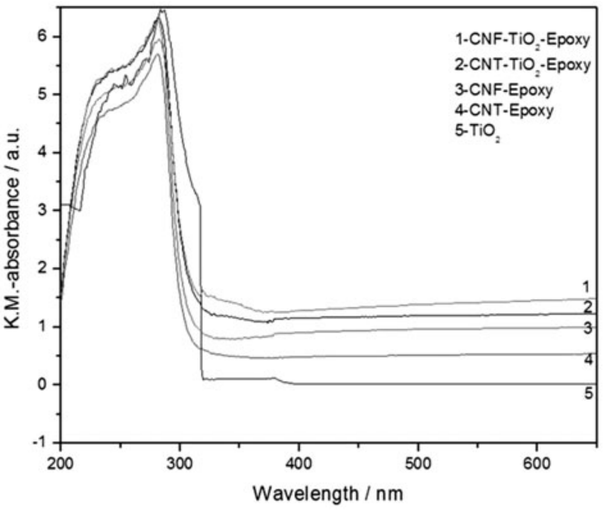

Fig. 2. DRUV–vis spectra of composite materials (1) CNF-TiO_2-Epoxy, (2) CNT-TiO_2-Epoxy, (3) CNF-Epoxy, (4) CNT-Epoxy and (5) TiO_2.

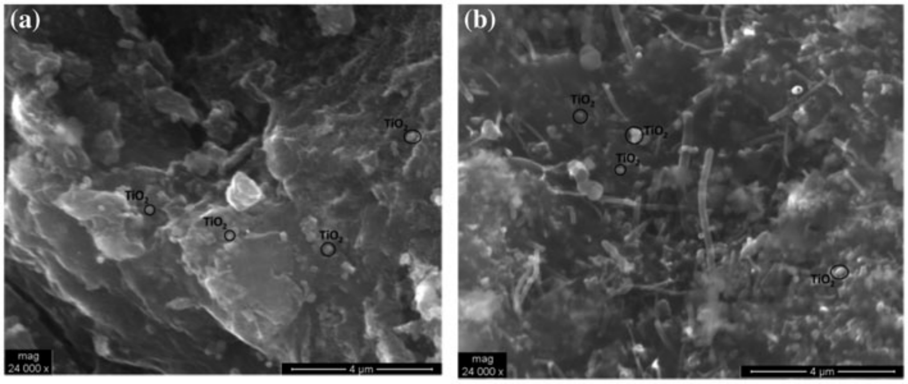

Fig. 1. SEM image of (a) CNT-TiO_2-Epoxy and (b) CNF-TiO_2-Epoxy.

VIS-driven applications are beyond our aim. No significant enhancement of absorption intensity in UV wavelength is noticed on CNT-TiO_2-Epoxy and CNF-TiO_2-Epoxy in comparison with TiO_2. However, the adsorption stage that represents the key for the photocatalytic application performance should be improved in the presence of the nanostructured carbon.

3.3. *Testing carbon-TiO_2 composite materials in adsorption and photocatalysis processes for HA removal from water*

The adsorption process for HA removal using all composite materials was characterized through kinetics and equilibrium studies.

3.3.1. *Adsorption-kinetics studies*

Zero, first and pseudo-second-order kinetics models were tested for fitting the experimental data. If the pseudo-second-order kinetics fitted well in the experimental data, the plot of t/q_t vs. t should show a linear relationship. Zero and first-order kinetics models were not appropriate for fitting the experimental data.

The linear plots of t/q_t vs. t (Fig. 3) show that the experimental data agree with the pseudo-second-order kinetic model for the HA adsorption. The calculated q_e values agree very well with the experimental data and the correlation coefficients for the second-order kinetic model are higher than 0.99 in almost all cases. These indicate that the adsorption of HA from water onto composite materials obeys the pseudo-second-order kinetic model that predicts an exponential decay of concentrations as a function of time. There are many experimental parameters, e.g. targeted organic compounds-type and concentration, catalyst dose and pH that control the reaction rate and kinetics.

Table 1
Results of fitting experimental data to pseudo-second-order kinetic model for 10 mg L^{-1} HA concentration

	Parameters		
Composite type	q_e (mg g^{-1})	k_2 (g mg^{-1} min^{-1})	R^2
CNT-TiO_2-Epoxy	8.6850	0.00963	0.9998
CNF-TiO_2-Epoxy	7.14438	0.00897	0.99175

Table 1 presents the kinetic parameters resulted by fitting the pseudo-second-order equation to the experimental data recorded for 10 mg L^{-1} HA, and it can be noticed that even if CNT-TiO_2-Epoxy exhibited higher equilibrium adsorption capacity (q_e) and also, the adsorption rate is slightly faster in comparison with CNF-TiO_2-Epoxy composite material.

3.3.2. *Adsorption—equilibrium studies*

The results of adsorption isotherm fitting using the three models showed that the Freundlich model fitted best in the adsorption data with good correlation coefficient ($R^2 > 0.99$). The results of Freundlich model fitting are presented in Fig. 4. The correlation coefficient values of $R^2 = 0.9518$ obtained for Langmuir and of $R^2 = 0.81$ for D–R model led to choose Freundlich model (Fig. 4) to describe the adsorption process. This

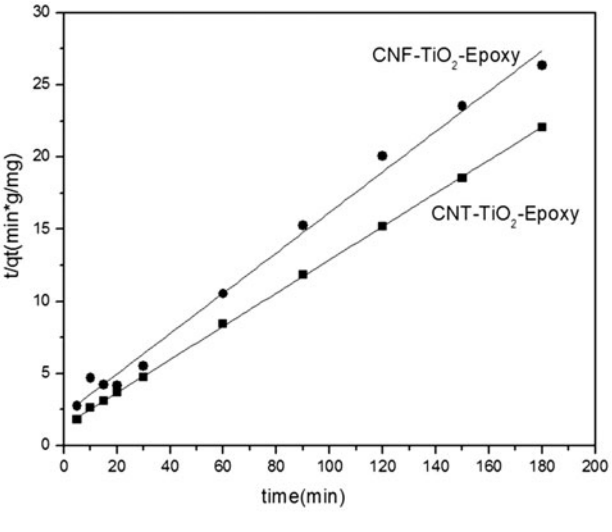

Fig. 3. The pseudo-second-order adsorption kinetic model for CNT-TiO_2-Epoxy and CNF-TiO_2-Epoxy.

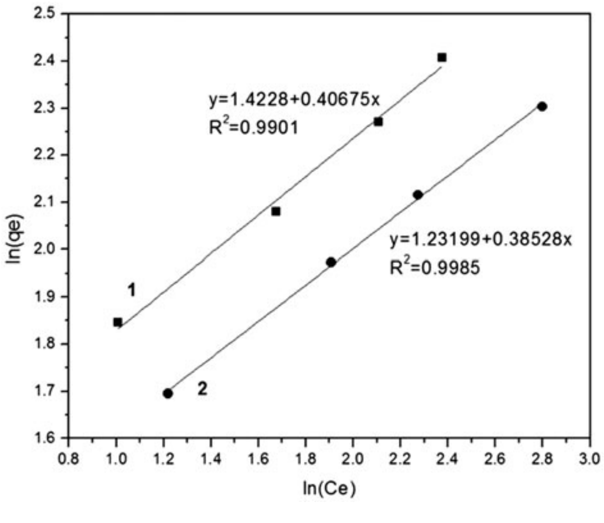

Fig. 4. Freundlich isotherm plot for the adsorption of HA on (1) CNT-TiO_2-Epoxy and (2) CNF-TiO_2-Epoxy.

model is an empirical one and applicable to the adsorption on heterogeneous surface. The first available sorption sites are occupied and characterized by the strong bindings that are weaker with increasing degree of sites occupation [11]. Based on the results presented in Table 2, it can be seen that the adsorption capacity was higher for CNT-TiO_2-Epoxy than for CNF-TiO_2-Epoxy. The Freundlich "*n*" values were similar for both sorbents suggesting the same adsorption affinities for HA.

In general, the adsorption mechanism on carbon-based adsorbents is considered to be complex based on the hydrophobic effect, electrostatic interactions, hydrogen bonding and π–π bonds [11]. Both CNTs and CNFs provide hydrophobic regions that interact strongly with hydrophobic fraction of HA, this can be considered as one of the important mechanism. Nevertheless, it has been proved that no hydrophobic effect was the dominant mechanism even under the conditions of strong affinity of CNT to organic chemicals [37]. To assess the electrostatic interactions, the electrokinetic Zeta potential (ζ) for each material at pH 6.5 was determined and the values are gathered in Table 3.

By corroboration the kinetics and equilibrium adsorption results with the Zeta potential values, it is noticed that no electrostatic interaction was a significant mechanism for HA adsorption. Even if the Zeta potential for all tested materials including HA is characterized by the negative value at this neutral pH of 6.5, except TiO_2 that is characterized by the isoelectric point, which means that the repulsion phenomenon is favoured; however, HA adsorption occurred the best for CNT-TiO_2-Epoxy and CNF-TiO_2-Epoxy.

The different adsorption capacity for HA of CNT-TiO_2-Epoxy and CNF-TiO_2-Epoxy could due to the morphology difference that may result in a difference in their aggregation tendency, which may further impact their adsorption ability by the less available active sites. Also, the adsorption capacity is influenced by the different porous structures and the more uniform pore structure favoured the diffusion of the pollutants in inner pores [11]. These peculiarities are reflected also in the specific surface area that is much higher for CNT vs. CNF. Ren et al. [38] reviewed the factors affecting the adsorptive interactions between organic pollutants and CNTs, as (i) nanostructured carbon peculiarities in relation with the surface area, size, shape pore diameter and volume, morphology, functional groups and impurity, (ii) organic molecule properties of hydrophobicity, polarity, size and functional group and (iii) operational conditions (pH, ionic strength).

To evidence more detailed the adsorption performances of both CNT-TiO_2-Epoxy and CNF-TiO_2-Epoxy the comparative adsorption studies vs. TiO_2, CNT-Epoxy and respective, CNF-Epoxy was performed for the adsorption of 25 mg L^{-1} HA. Fig. 5 shows the adsorption efficiency expressed in terms of efficiency degree (%). It is obviously that CNTs-based composite material exhibited higher adsorption ability for HA in comparison with CNFs-based composite material, which is expected in relation with the higher specific surface area for CNT. Different adsorption

Table 2
Freundlich isotherm parameters of HA adsorption on CNT-TiO_2-Epoxy (1) and CNF-TiO_2-Epoxy (2)

Material	K_F (L g^{-1})	*n*	R^2
CNT-TiO_2-Epoxy	0.24103	0.40675	0.9901
CNF-TiO_2-Epoxy	0.29171	0.38528	0.9985

Table 3
Zeta potential (ζ)

Material	ζ potential/mV
CNF-Epoxy	−26.585
CNF-TiO_2-Epoxy	−32.314
CNT-Epoxy	−10,334
CNT-TiO_2-Epoxy	−22.655
TiO_2	0
Humic acid solution (25 mg L^{-1})	−32.5

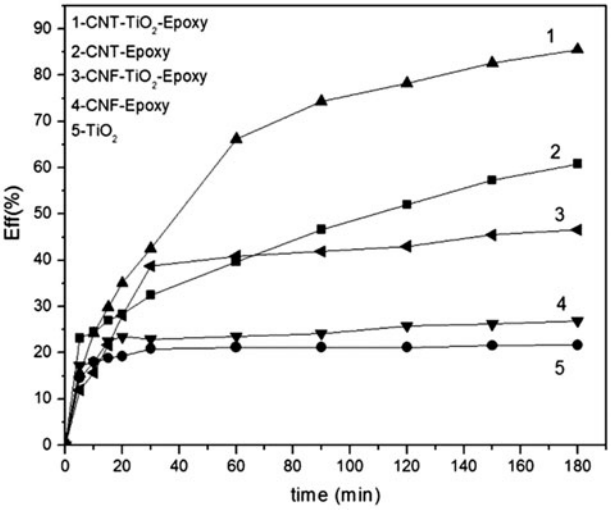

Fig. 5. Evolution of HA removal efficiency in time by adsorption on CNT-TiO_2-Epoxy (1); CNT-Epoxy (2); CNF-TiO_2-Epoxy (3); CNF-Epoxy (4); TiO_2 (5).

behaviour is evidenced for CNTs that reached the equilibrium after longer time in comparison with CNFs composite and TiO_2. This behaviour should be explained by more porous structure for CNTs. The presence of TiO_2 gave its contribution to the adsorption of HA onto composite system.

3.3.3. Photocatalytic activity of the composite materials

The photocatalytic activities of the composite materials were assessed for the degradation of HA for comparison with the sorption performances. The photocatalysis results expressed in terms of HA amount removed per unit of TiO_2 are shown in Fig. 6. It must be mentioned that the photocatalysis component is assessed by subtracting adsorption results from overall photocatalysis process. It can be noticed that the best photocatalysis results are achieved for CNT-TiO_2-Epoxy composite, especially in the first stage of photocatalysis process. However, after 1,80 min of irradiation, HA degraded in the presence of CNT-TiO_2-Epoxy composite is slightly better than in the presence of TiO_2. Similar behaviour was shown for CNFs-based composite materials, for which photocatalysis performance was worse in comparison with CNTs. This behaviour informed about a possible self-photocatalytic activity of carbonaceous in according with the literature data [39]. Also, as we mentioned previously the adsorption stage that represents the key of adsorption process was improved.

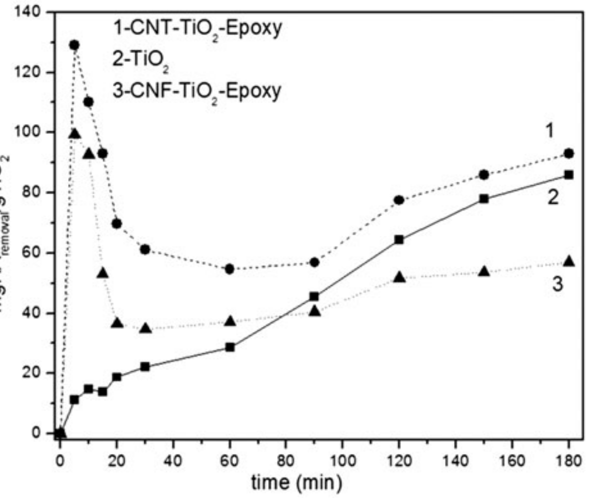

Fig. 6. Evolution of HA removed by photocatalysis under UV irradiation normalized per TiO_2 unit vs. time using (1) CNT-TiO_2-Epoxy, (2) TiO_2 and (3) CNF-TiO_2-Epoxy.

The kinetics results determined by the Langmuir–Hinshelwood kinetic model expressed as the apparent first-order rate constant (k_{app}) [40] are gathered in Table 4, and it can be seen that the fastest rate of HA degradation by photocatalysis under UV irradiation was achieved for CNT-TiO_2-Epoxy composite material.

To assess if the photocatalytic activity of the composite is enhanced should compare with a standard that is TiO_2 unit. The effect can be quantified in terms of the enhancement factor (R) defined by Eq. (8):

$$R = \frac{k'_{\text{app}}\text{composite}}{k'_{\text{TiO}_2}} \tag{8}$$

where k'_{app} is apparent first-order rate constant normalized per TiO_2 unit.

The enhancement factor of about 10 was achieved for CNT-TiO_2-Epoxy and about 5 for CNF-TiO_2-Epoxy composite. Based on these results, it can be concluded about the enhanced performance of the nanostructured carbon-TiO_2-epoxy system in special for CNTs. Taking into account the morpho-structural aspects of the composite and the literature data reported for carbon nanotube-TiO_2 composite [31], the photocatalysis mechanism is very complex. Nanostructured carbon and TiO_2 particles are distributed as small islands within insulating matrix, part of them being attached one by other. Thus, part of them should acts as individual photocatalyst and other by the two mechanism described by Woan et al. [31]. One mechanism

Table 4
Apparent rate constants for photocatalytic degradation of 25 mg L^{-1} HA solution by UV irradiation

Composite type	k_{app} (min^{-1})	k'_{app} (min^{-1} g^{-1} TiO_2)	R^2
CNT-TiO_2-Epoxy	0.01996	0.4990	0.98565
CNT-Epoxy	0.01152		0.94603
CNF-TiO_2-Epoxy	0.0104	0.2600	0.98962
CNF-Epoxy	0.0077		0.8684
TiO_2	0.00921	0.0460	0.92885

supposes the sink function of the nanostructured carbon for the electron from TiO_2 conduction band avoiding the electron–hole recombination. Another is based on the generation of the electron-hole pair in the nanostructured carbon that was proved by DRUV–VIS characterization results.

Because no pronounced enhanced HA, degradation in terms of efficiency was achieved by the photocatalysis in comparison with the adsorption using nanostructured carbon-based composite materials, the lifetime of the CNT-TiO_2-Epoxy composite material as sorbent and as photocatalyst was assessed by repetitive five running in sorption and photocatalysis processes. The HA removal efficiency after 1,80 min reached by applying the adsorption and photocatalysis processes are presented in Fig. 7. It can be noticed that by photocatalysis the material fouling is slowed in comparison with its application in sorption process. In addition, a regeneration step of the material was tested by applying the photocatalysis under the same conditions, but only in water without HA presence and then, by further photocatalysis application for HA degradation a better efficiency was achieved. However, no complete regeneration was achieved by this method because HA degradation efficiency was about 56.15% for regenerated material vs. 81.63% HA degradation efficiency reached by the first utilization.

This composite may provide a robust system requiring little maintenance, which exhibits a great potential application in water decontamination as next generation of self-cleaning filtering material.

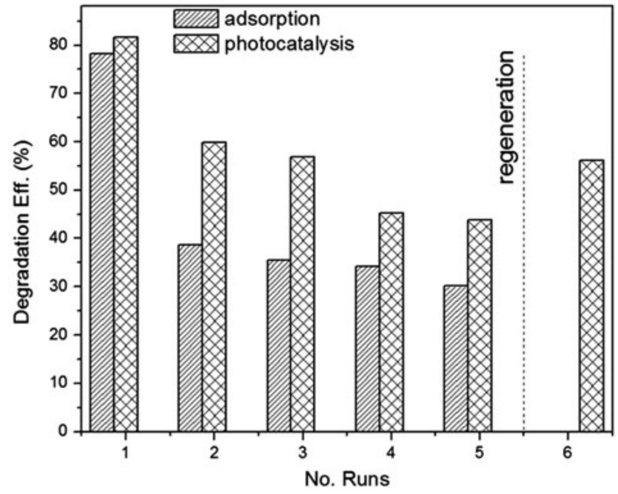

Fig. 7. Evolution of HA removal degree during successive running of comparative photocatalytic and adsorption process on CNT-TiO_2-Epoxy for 25 mg L^{-1} HA without/with regeneration.

4. Conclusions

Two types of nanostructured carbon-TiO_2 within epoxy matrix, i.e. carbon nanotubes-titanium dioxide-epoxy (CNT-TiO_2-Epoxy) and carbon nanofibers-titanium dioxide-epoxy (CNF-TiO_2-Epoxy) have been prepared, characterized and tested as sorbent and photocatlysts for HAs removal envisaging advanced drinking water treatment. The adsorption capacities of CNT-TiO_2-Epoxy of 8.68 mg g^{-1} and CNF-TiO_2-Epoxy of 7.14 mg g^{-1} for HA were determined using Freundlich isotherm. The different adsorption capacity own the morphology and porosity difference between CNTs and CNFs, which is reflected in specific surface area and also, may affect their aggregation tendency that may further impact their adsorption ability. The presence of TiO_2 into composite composition contributed to the adsorption process related to its distribution within epoxy matrix or its attachment onto nanostructured carbon surface. The photocatalytic activities of both composite materials were assessed comparatively with TiO_2 reference photocatalyst. Besides the role of the nanostructured carbon in adsorption step considered as the key for the photocatalysis performance, it was found that both CNTs and CNFs exhibited photocatalytic properties. The most enhanced photocatalytic performance for HA degradation was achieved for CNT-TiO_2-Epoxy composite material, while for CNF-TiO_2-Epoxy the photocatalytic performance was slightly worse in comparison with TiO_2, which should be explained by a potential blockage of the photoactive centers in TiO_2 after its immobilization together CNFs within epoxy matrix.

The lifetime and the regeneration pathway by the photocatalysis investigated for CNT-TiO_2-Epoxy composite system showed a HA removal efficiency of 43.8% achieved by photocatalysis vs. 30.2% reached by the sorption after successive five running. A regeneration degree of about 25% was achieved under the similar conditions of photocatalysis without HA presence, which showed that the photocatalysis method is suitable as regeneration step for application of CNT-TiO_2-Epoxy as sorbent and/or photocatalyst for HA removal from water envisaging the advanced drinking water treatment. For concrete practical application in advanced drinking water treatment technology this CNT-TiO_2-Epoxy composite-based robust system should be used as attractive addition or alternative to the various oxidation/filtering techniques that are currently used.

Acknowledgements

This work was supported by the Romanian National Research Programs PN-II-ID-165/2011 and PNII-60/2012.

References

[1] M.A. Ferro-García, J. Rivera-Utrilla, I. Bautista-Toledo, C. Moreno-Castilla, Adsorption of humic substances on activated carbon from aqueous solutions and their effect on the removal of Cr(III) ions, Langmuir 14 (1998) 1880–1886.

[2] W.W. Tang, G.M. Zeng, J.L. Gong, J. Liang, P. Xu, C. Zhang, B.B. Huang, Impact of humic/fulvic acid on the removal of heavy metals from aqueous solutions using nanomaterials: A review, Sci Total Environ. 468–469 (2014) 1014–1027.

[3] A. Kerc, M. Bekbolet, A.M. Saatci, Effect of partial oxidation by ozonation on the photocatalytic degradation of humic acids, Int. J. Photoenergy 5 (2003) 75–80.

[4] X.Z. Li, C.M. Fan, Y.P. Sun, Enhancement of photocatalytic oxidation of humic acid in TiO_2 suspensions by increasing cation strength, Chemosphere 48 (2002) 453–460.

[5] K. Kadirvelu, C. Karthika, N. Vennilamani, S. Pattabhi, Activated carbon from industrial solid waste as an adsorbent for the removal of Rhodamine-B from aqueous solution: Kinetic and equilibrium studies, Chemosphere 60 (2005) 1009–1017.

[6] Q. Wang, D. Yang, D. Chen, Y. Wang, Z. Jiang, Synthesis of anatase titania-carbon nanotubes nanocomposites with enhanced photocatalytic activity through a nanocoating-hydrothermal process, J. Nanopart. Res. 9 (2007) 1087–1096.

[7] Z.P. Luo, J.H. Koo, Quantitative study of the dispersion degree in carbon nanofiber/polymer and carbon nanotube/polymer nanocomposites, Mater. Lett. 62 (2008) 3493–3496.

[8] C. Orha, A. Pop, C. Lazau, A. Jakab, R. Pode, F. Manea (Eds.), Water Contamination Emergencies: Managing the Threats, Royal Society of Chemistry, Cambridge, 2013, pp. 346–355.

[9] P. Le-Clech, E.K. Lee, V. Chen, Hybrid photocatalysis/membrane treatment for surface waters containing low concentrations of natural organic matters, Water Res. 40 (2006) 323–330.

[10] J. Heo, H. Kim, N. Her, S. Lee, Y.G. Park, Y. Yoon, Natural organic matter removal in single walled carbon nanotubes-ultrafiltration membrane systems, Desalination 298 (2012) 75–84.

[11] X. Liu, M. Wang, S. Zhang, B. Pan, Application potential of carbon nanotubes in water treatment: A review, J. Environ. Sci. 25(7) (2013) 1263–1280.

[12] D. Li, H. Haneda, Photocatalysis of sprayed nitrogen-containing Fe_2O_3–ZnO and WO_3–ZnO composite powders in gas-phase acetaldehyde decomposition, Photochem. Photobiol. Chem. 160 (2003) 203–212.

[13] N. Takeda, N. Iwata, T. Torimoto, H. Yoneyama, Influence of carbon black as an adsorbent used in TiO_2 photocatalyst films on photodegradation behaviors of propyzamide, J. Catal. 177 (1998) 240–246.

[14] V. Georgakilas, D. Gournis, V. Tzitzios, L. Pasquato, D.M. Guldi, M. Prato, Decorating carbon nanotubes with metal or semiconductor nanoparticles, J. Mater. Chem. 17 (2007) 2679–2694.

[15] M. Knite, V. Tupureina, A. Fuith, J. Zavickis, V. Teteris, Polyisoprene-multi-wall carbon nanotube composites for sensing strain, Mater. Sci. Eng. C 27 (2007) 1125–1128.

[16] J.M. Lee, K. Palanivelu, Y.S. Lee, Removal of hexavalent chromium on chitosan-deposited activated carbon, Solid State Phenom. 135 (2008) 85–88.

[17] B. Gao, C. Peng, G.Z. Chen, G.L. Lipuma, Photo-electro-catalysis enhancement on carbon nanotubes/titanium dioxide (CNTs/TiO_2) composite prepared by a novel surfactant wrapping sol–gel method, Appl. Catal. B.-Environ. 85 (2008) 17–23.

[18] W. Wang, P. Serp, P. Kalck, C. Silva, J.L. Faria, Preparation and characterization of nanostructured MWCNT-TiO_2 composite materials for photocatalytic water treatment applications, Mater. Res. Bull. 43 (2008) 958–967.

[19] P. Vincent, A. Brioude, C. Journet, S. Rabaste, S.T. Purcell, J. Le Brusq, J.C. Plenet, Inclusion of carbon nanotubes in a TiO_2 sol–gel matrix, J. Non-Cryst. Solids 311 (2002) 130–137.

[20] K. Hernadi, E. Ljubović, J.W. Seo, L. Forró, Synthesis of MWNT-based composite materials with inorganic coating, Acta Mater. 51 (2003) 1447–1452.

[21] B. Gao, G.Z. Chen, G.L. Li Puma, Carbon nanotubes/titanium dioxide (CNTs/TiO_2) nanocomposites prepared by conventional and novel surfactant wrapping sol–gel methods exhibiting enhanced photocatalytic activity, Appl. Catal. B.-Environ. 89 (2009) 503–509.

[22] B. Ahmmad, Y. Kusumoto, S. Somekawa, M. Ikeda, Carbon nanotubes synergistically enhance photocatalytic activity of TiO_2, Catal. Commun. 9 (2008) 1410–1413.

[23] W. Wang, P. Serp, P. Kalck, J.L. Faria, Photocatalytic degradation of phenol on MWNT and titania composite catalysts prepared by a modified sol–gel method, Appl. Catal. B. Environ. 56 (2005) 305–312.

[24] G. Hu, X. Meng, X. Feng, Y. Ding, S. Zhang, M. Yang, Anatase TiO_2 nanoparticles/carbon nanotubes nanofibers: preparation, characterization and photocatalytic properties, J. Mater. Sci. 42 (2007) 7162–7170.

[25] S. Aryal, C.K. Kim, K.-W. Kim, M.S. Khil, H.Y. Kim, Multi-walled carbon nanotubes/TiO_2 composite nanofiber b, electrospinning, Mater. Sci. Eng. C 28 (2008) 75–79.

[26] J. Cho, S. Schaab, J.A. Roether, A.R. Boccaccini, Nanostructured carbon nanotube/TiO_2 composite coatings using electrophoretic deposition (EPD), J. Nanopart. Res. 10 (2008) 99–105.

[27] H. Yu, X. Quan, S. Chen, H. Zhao, TiO_2-multiwalled carbon nanotube heterojunction arrays and their charge separation capability, J. Phys. Chem. C 111 (2007) 12987–12991.

[28] E. Traversa, M.L.D. Vona, P. Nunziante, S. Licoccia, T. Sasaki, N. Koshizaki, Sol–Gel preparation and characterization of Ag–TiO_2 nanocomposite thin films, J. Sol–Gel Sci. Technol. 19 (2000) 733–736.

[29] R. Suárez-Parra, I. Hernández-Pérez, M.E. Rincón, S. López-Ayala, M.C. Roldán-Ahumada, Visible light-induced degradation of blue textile azo dye on TiO_2/

CdO-ZnO coupled nanoporous films, Solar Energy Mater. Solar Cells 76 (2003) 189–199.

[30] S.-J. Kim, J.-S. Im, P.-H. Kang, T.-J. Kim, Y.-S. Lee, Photocatalytic activity of CNT-TiO_2 nanocomposite in degrading anionic and cationic dyes, Carbon Lett. 9 (2008) 294–297.

[31] K. Woan, G. Pyrgiotakis, W. Sigmund, Photocatalytic carbon-nanotube–TiO_2 composites, Adv. Mater. 21 (2009) 2233–2239.

[32] Z. Lin, L. Ji, X. Zhang, Electroanalytic properties of Pt/carbon composite nanofibers, Electrochem. Acta 54 (2009) 7042–7047.

[33] R. Leary, A. Westwood, Carbonaceous nanomaterials for the enhancement of TiO_2 photocatalysis, Carbon 49 (2011) 741–772.

[34] C. Lazau, C. Ratiu, C. Orha, R. Pode, F. Manea, Photocatalytic activity of undoped and Ag-doped TiO_2-supported zeolite for humic acid degradation and mineralization, Mater. Res. Bull. 46 (2011) 1916–1921.

[35] Y.S. Ho, G. McKay, Pseudo-second order model for sorption processes, Process Biochem. 34 (1999) 451–465.

[36] A.K. Gupta, A. Pal, C. Sahoo, Photocatalytic degradation of a mixture of Crystal Violet (Basic Violet 3) and Methyl Red dye in aqueous suspensions using Ag^+ doped TiO_2, Dyes Pigments 69 (2006) 224–232.

[37] K. Yang, L.Z. Zhu, B.S. Xing, Adsorption of polycyclic aromatic hydrocarbons by carbon nanomaterials, Enviro. Sci. Technol. 40 (2006) 1855–1861.

[38] X. Ren, C. Chen, M. Nagatsu, X. Wang, Carbon nanotubes as adsorbents in environmental pollution management: A review, Chem. Eng. J. 170 (2011) 395–410.

[39] L.F. Velasco, J.B. Parra, C.O. Ania, Role of activated carbon features on the photocatalytic degradation of phenol, Appl. Surf. Sci. 256 (2010) 5254–5258.

[40] J. Matos, J. Lain, J.-M. Herrmann, Association of activated carbons of different origins with titania in the photocatalytic purification of water, Carbon 37 (1999) 1870–1872.